Photothermal deflection spectra of solid C_{60}

1996 J. Phys.: Condens. Matter 8 5793

(http://iopscience.iop.org/0953-8984/8/31/012)

J. Phys.: Condens. Matter **8** (1996) 5793–5800. Printed in the UK

Photothermal deflection spectra of solid C_{60}

Wei-ya Zhou†, Si-shen Xie†, Sheng-fa Qian†, Gang Wang† and Lu-xi Qian‡

† Institute of Physics, Chinese Academy of Sciences, Beijing 100080, People's Republic of China

‡ Department of Physics, The Central University of Nationality, Beijing 100087, People's Republic of China

Received 25 March 1996, in final form 9 May 1996

Abstract. The optical absorption spectra of C_{60} single crystal and thin film in the weak-absorption region have been measured by photothermal deflection spectroscopy. The optical energy gaps, corresponding to optically forbidden transitions of weak absorption, were derived from Tauc plots. On comparison with the photothermal deflection spectrum of an amorphous semiconductor, the similarity suggests that the gap region of solid C_{60} can be described in terms used for amorphous semiconductors such as an Urbach edge and sub-gap defect absorption. The weak-absorption characteristics of solid C_{60} are discussed.

1. Introduction

The unique properties and potential applications of molecular C_{60} have been exciting a vast number of studies on the preparation of pure samples and the characterization of their chemical and physical properties. The optical absorption of the material also attracts considerable interest [1–9], because it not only provides a characteristic signature but also contains a wealth of information about the energy levels and the electron density of states. However, the reports on ultraviolet–visible (UV/VIS) optical spectra are limited other than for dissolved molecules [1–3] and polycrystalline thin films [4–6], mainly due to the difficulty of preparing flat thin crystals suitable for optical transmission measurements. A few investigations have been performed on the weak-absorption spectra [7–9], since it is difficult to determine the absorption ranging from the near infrared to the visible for solid C_{60}.

Pure crystalline C_{60} has a face-centred cubic (fcc) structure at room temperature. The C_{60} molecules are brought together by van der Waals forces and weak Coulomb interaction. Theoretically the undoped C_{60} crystal can be described as a narrow-band semiconductor with the energy gap between the highest occupied molecular orbital and lowest unoccupied molecular orbital (HOMO–LUMO) of 1.5–2.6 eV [10–12], which is optically forbidden. Various experiments, however, gave different values of the energy gap ranging from 1.5 to 2.3 eV [13–15]. Therefore, further investigations on the weak-absorption spectra of high-quality C_{60} single crystal are indispensable for understanding the delicate molecular interaction in solid C_{60}. Since the conventional transmission and reflectivity spectroscopies are not suitable for a sample with weak absorption due to their minimum detectable absorption of 10^{-2}, photothermal deflection spectroscopy (PDS) has been used in our work. PDS is well known as an advanced technique for its highly sensitive and nondestructive determination of the optical absorption of solid, liquid or gas based on the photothermal

0953-8984/96/315793+08$19.50

effect. In this paper, the weak-absorption spectra of both C_{60} thin film and single crystal grown by different methods are measured by means of PDS, and compared with those of an amorphous semiconductor film. The weak-absorption characteristics of solid C_{60} are discussed.

2. Experimental details

2.1. Preparation of thin films

The C_{60} powder with purity of 99.9% was kept in an evacuated quartz tube at about 523 K for 15 h in order to remove residual solvents used during the separation or purification process. This pre-treated C_{60} powder was sublimated in a quartz furnace at 735 K onto clean quartz substrates (1 cm $\times$ 0.5 cm, 0.8 mm in thickness) held at 415 K during deposition in a vacuum of 10^{-7} Torr. A typical flux rate for C_{60} deposition was about 3 nm min^{-1}. The shutter over the substrate was closed while the temperatures of the source and substrates were rising. The thickness of the C_{60} film was measured with a Dektak IIA profilometer. Raman and infrared (IR) spectra confirmed that the thin films obtained consisted almost entirely of polycrystalline C_{60}. The crystal structure of C_{60} thin films was face-centred cubic (fcc) as indicated by x-ray diffraction.

2.2. Growth of single crystals

Single crystals of C_{60} were prepared in two different ways: by the sublimation method and by the solution method. From the sublimation method [16], single crystals with fcc structure were obtained. Alternatively, from the CS_2 solution orthorhombic single crystals of C_{60} were grown [17]. Several flat-shaped fcc single crystals ($\sim$1.5 cm $\times$ 1 cm) with thicknesses of about 100 μm, 230 μm and 0.5 mm were selected for PDS measurements. An orthorhombic C_{60} single crystal ($\sim$1 mm $\times$ 0.4 mm) with a thickness of about 0.1 mm was used in the PDS measurements.

2.3. Measurements

The strong UV/VIS transitions of C_{60} thin films were measured using a CARY 2390 UV/VIS/NIR spectrophotometer. The scanning rate was 1 or 0.5 nm s^{-1}.

The weak-absorption spectra of C_{60} single crystals and thin films below 2.3 eV (540 nm) were determined by transverse photothermal deflection spectroscopy (PDS). A xenon arc lamp with a monochromator was used as an exciting light source (pump beam), and the focused beam was modulated by a mechanical chopper. The probe beam was a 0.5 mW He–Ne laser. The amplitude and phase of the probe beam deflection were detected with a highly sensitive position sensor, and fed into the (A–B) input of a lock-in amplifier. The detected PDS signal must be normalized by the intensity spectrum of a pump beam with a modulation frequency of 10 Hz. Additional details about the PDS are given in [18, 19]. Because of the high sensitivity of PDS it is possible to measure forbidden transitions as well as defect states that would not be detected by other techniques. The measurements were performed at room temperature. Silicone oil was selected as a deflection medium.

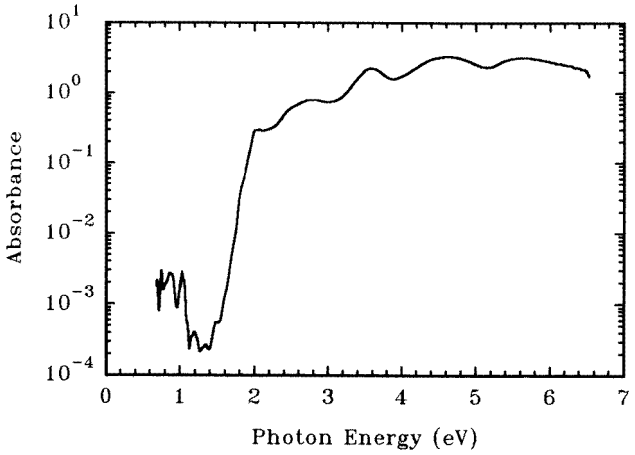

Figure 1. Optical absorption of a C_{60} thin film. In the region around 2.1 eV the PDS and transmission data are overlapped after normalization.

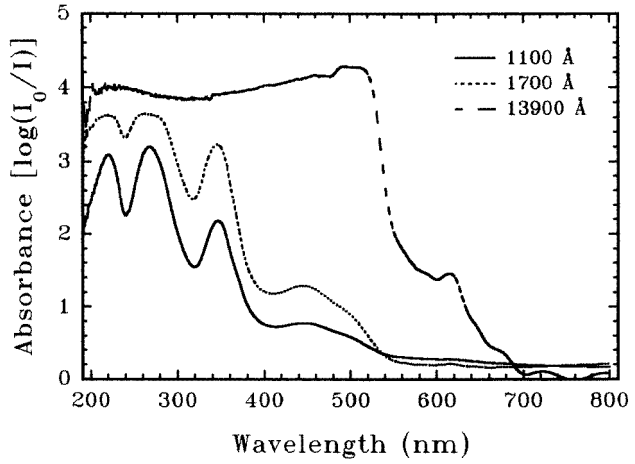

Figure 2. UV/VIS spectra of three C_{60} films: ——, 1100 Å; ·····, 1700 Å; - - - -, 13 900 Å.

3. Results and discussion

The full optical absorption spectrum of C_{60} thin film is shown in figure 1, which is obtained by overlapping the PDS data with the optical transmission data in the region around 590 nm (2.1 eV) where the former is near saturation while the latter is near the resolution limit. The UV/VIS spectra above the gap region (6.5–2.3 eV) are easily determined by the conventional optical transmission method. The absorbance is shown in figure 2 for three thin films (solid line: 1100 Å; dotted line: 1700 Å; dashed line: 13 900 Å). The features reproduce details measured by other people [4–6]. Strong absorption peaks occur at 220 nm (5.636 eV), 268 nm (4.627 eV), and 346 nm (3.584 eV), respectively. An obvious shoulder at 500 nm (2.48 eV) is observed near the middle strong peak at 445 nm (2.787 eV). At 616 nm (2.013 eV), a weak peak can be found. According to the electronic structure of the C_{60}

molecule [20], the symmetry-allowed transitions corresponding to the absorption peaks may be assigned as $H_u \rightarrow T_{1g}$ 2.787 eV, $H_g \rightarrow T_{1u}$ 3.584 eV, $H_u \rightarrow H_g$ 4.627 eV and G_g, $H_g \rightarrow T_{2u}$ 5.636 eV. Since the HOMO–LUMO dipole transition is a symmetrically forbidden one with weak absorption, it is difficult to estimate the value of the energy gap directly from figure 2. For the near-gap (2.3–1.6 eV) and the sub-gap (below 1.6 eV) regions, therefore, PDS was used for investigating the interesting weak absorption for both thin films and single crystals of C_{60}.

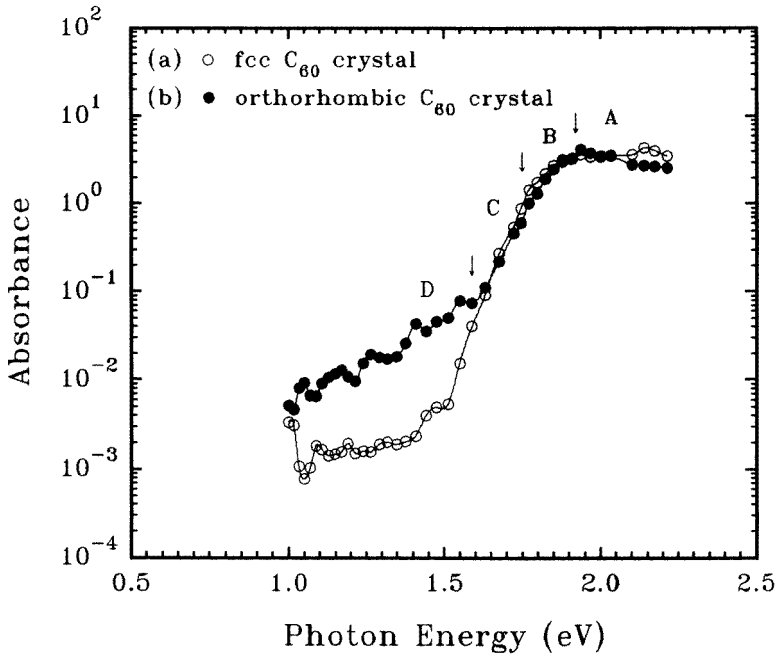

Figure 3. Visible and near-IR spectra of C_{60} single crystals determined by PDS. The arrows denote the boundaries of the regions A, B, C and D: (a) fcc C_{60} single crystal; (b) orthorhombic C_{60} single crystal.

The PDS spectra of a fcc and an orthorhombic C_{60} single crystal are shown in figure 3 as (a) and (b), respectively, and that of a fcc C_{60} thin film with the thickness of 1.4 μm is shown in figure 4 as (a). The spectrum can be divided into four regions: A, B, C and D, as shown in figure 3. The arrows in figure 3 denote the boundaries of the regions A, B, C and D. In region A, the energy is above the energy gap and the optical absorption spectra can be measured by a conventional transmission method such as is shown in figure 2. Region B, where the absorption coefficient, α, is proportional to the power of the energy of incident photons, $h\nu$, is called a 'high'-absorption region. Region C is an 'exponential' absorption region, where α is proportional to the exponent of $h\nu$. Region D denotes the 'sub-gap' absorption dominated by transitions from extended valence band states to defect states or from defect states to extended conduction band states. Here, regions B and C are classified as 'near-gap' absorption region.

For region B, the PDS spectra ($h\nu \sim 1.75$–1.9 eV) for two kinds of single crystal grown by different methods are coincident (shown in figure 3), while the corresponding energy ($h\nu \sim 1.85$–2.05 eV) for a C_{60} thin film in figure 4, (a), is about 0.1 eV higher than that

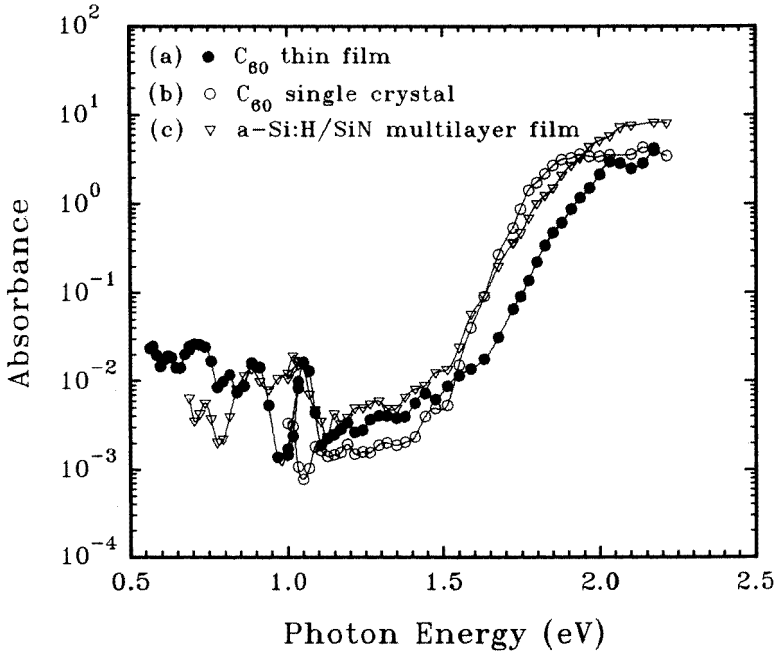

Figure 4. Visible and near-IR spectra of C_{60} thin films and single crystals as well as a-Si:H/SiN multilayer film determined by PDS: (a) fcc C_{60} thin film; (b) fcc C_{60} single crystal; (c) a-Si:H/SiN multilayer film.

of pure fcc C_{60} single crystal. This means that the energy gap of pure C_{60} single crystal would be about 0.1 eV narrower than that of C_{60} thin film.

The spectra of solid C_{60} are similar to those of amorphous semiconductor films. In order to make a comparison, the absorption spectrum of an amorphous silicon/silicon nitride multilayer film (a-Si:H/SiN, 1.6 μm thickness) was measured by PDS, and also shown in figure 4 as (c). For region A in the spectra of the solid C_{60}, therefore, the optical gaps can be derived by using the Tauc equation [21] which is usually adopted for amorphous semiconductors:

$$(\alpha h\nu)^{1/2} = B(h\nu - E_{\mathrm{opt}}) \tag{1}$$

where E_{opt} is the optical energy gap, $h\nu$ is the energy of the incident light and B is a constant related to the properties of the material.

Table 1. Values of E_{opt} derived from Tauc plots (eV).

Sample	fcc C_{60} crystal	Orthorhombic C_{60} crystal	fcc C_{60} thin film	a-Si:H/SiN multilayer film
$(\alpha h\nu)^{1/2}$	1.63	1.65	1.75	1.69

Figures 5(a)–5(d) show the Tauc plots for a fcc C_{60} single crystal, an orthorhombic C_{60} single crystal, a fcc C_{60} thin film and an a-Si:H/SiN multilayer film, respectively. The values of E_{opt} derived from the Tauc plots are listed in table 1. Because each plot corresponds to

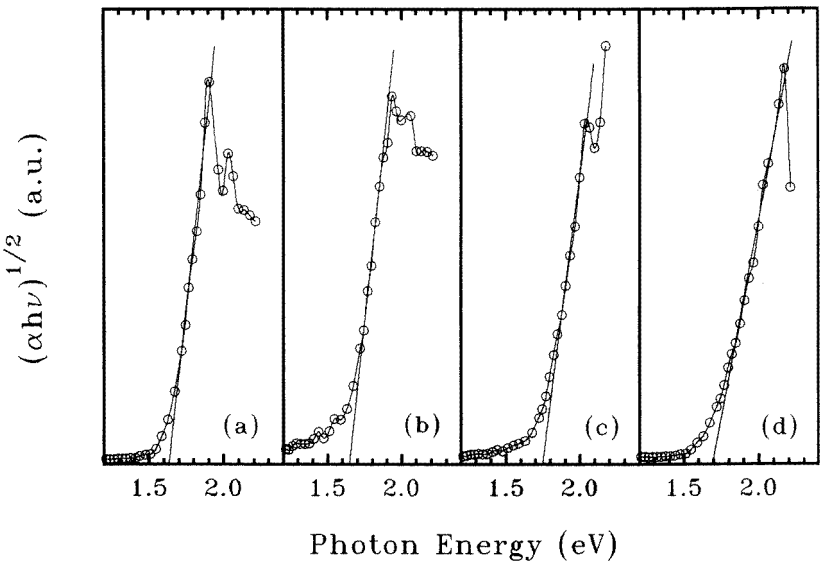

Figure 5. Tauc plots for various samples: (a) fcc C_{60} single crystal; (b) orthorhombic C_{60} single crystal; (c) fcc C_{60} thin film; (d) a-Si:H/SiN multilayer film.

a straight line over a large energy region, the plot for equation (1) can be reasonably used to estimate E_{opt} for solid C_{60} as it is for an a-Si:H/SiN multilayer film.

By comparison of the PDS spectra (a) and (b) in figure 4, it is observed that the optical absorption edge of fcc C_{60} single crystal is shifted to an energy about 0.1 eV lower with respect to that of C_{60} thin film. Generally, the sub-gap and above-gap absorptions are related to the short-range order and long-range order of the phonon in the semiconductors [8], respectively. Better long-range order can be found in fcc C_{60} single crystals than in thin films by high-resolution transmission electron microscopy and x-ray diffraction analysis, although these two kinds of sample have the same fcc structure and the C_{60} molecules gather due to van der Waals forces. It is the difference in the phonon state densities that causes the optical energy gap of the pure C_{60} single crystal to be narrower than that of the thin film.

Various experimental studies have given different energy gaps for C_{60} solids, e.g., 1.5–2.0 eV from ultraviolet photoelectron spectroscopy [13], 1.8 eV from electron energy-loss spectroscopy [14], 1.5 eV from optical absorption [7], and 2.3 eV from photoelectron spectroscopy and inverse photoelectron spectroscopy [15]. The HOMO–LUMO energy gaps calculated by various kinds of method are 1.5–2.6 eV [10–12]. Saito and Oshiyama [12] reported, using a local density approximation, that the energy gap between the H_u (HOMO) state and the T_{1u} (LUMO) state was about 1.9 eV for the C_{60} cluster, and that the band gap of solid C_{60} with fcc structure was calculated to be about 1.5 eV. Because the group theory analysis indicated that the HOMO–LUMO transition is a dipole-forbidden one, the energy gaps of pure C_{60} single crystals and thin films would be smaller than the values of E_{opt} derived from the present PDS measurement (1.63 eV and 1.75 eV, respectively). Due to the disorder effect, however, the energy gap of solid C_{60} might be close to E_{opt}, since in this case there would be no restriction on the lowest optical transition due to dipole selection rules.

Table 2. Urbach energies (meV).

Sample	fcc C_{60} crystal	Orthorhombic C_{60} crystal	fcc C_{60} thin film	a-Si:H/SiN multilayer film
U (meV)	48	72	62	69

The disorder in solid C_{60} can be represented by the Urbach energy, which is exhibited in the PDS. It is the disorder that results in the difficulty of determination of the energy gap for solid C_{60}. For region C in figures 3 and 4, the relation between α and $h\nu$ can be characterized by the expression

$$\alpha = \alpha_0 \exp(h\nu/U) \tag{2}$$

where U is the 'Urbach energy' which is interpreted as a broadening of the intrinsic absorption edge due to disorder and related to the transitions from the extended valence band states to the localized states at the conduction band tail. The larger the value of U, the greater the compositional, topological, or structural disorder. The Urbach energies (listed in table 2) are 48, 72 and 62 meV for a fcc C_{60} single crystal, an orthorhombic C_{60} single crystal and a fcc C_{60} thin film, respectively, which are comparable to the value of 69 meV obtained for an a-Si:H/SiN multilayer film. The fcc C_{60} single crystal has a smaller Urbach value than C_{60} thin film, which gives further proof of the lower degree of disorder in the fcc C_{60} single crystal. There are several possible origins for the disorder in solid C_{60}: (1) the surface is contaminated inevitably by impurities or intercalated by oxygen, since the sample has been exposed to air for a time; (2) it is easy to produce structural defects such as stacking faults or irregularly oriented microcrystal boundaries during crystal growth and especially in preparation of thin film; and (3) since the molecules of C_{60} rotate substantially at room temperature, domains could be introduced which might destroy the long-range order. It is these disorders that may give rise to the band-tail and sub-gap defect states.

The absorption behaviour below 1.6 eV, i.e. in sub-gap region D in figure 3 and figure 4, is more complicated. Although the optical energy gaps are coincident for the fcc and the orthorhombic C_{60} single crystals (figure 3), the sub-gap states in (b) in figure 3 might be influenced greatly by intercalation such as with the solvent or impurities. In region D of figure 3 and (a) in figure 4 the absorption shoulder at about 1.45 eV might be attributed to the transition between sub-gap states, which reflects the density and distribution of sub-gap states.

Absorption below 1.4 eV may be substantially influenced by C–H and O–H overtones. In order to further elucidate this feature, we have measured the PDS of the quartz substrate using alcohol and silicone oil as the deflection media, respectively, and also measured the PDS of various samples in these deflection media. It is observed that the absorption of solid C_{60} is covered on the whole by the absorption of silicone oil below 1.1 eV, while the influences of the medium upon the absorption of C_{60} film in the near-gap region could be neglected in the present PDS measurement.

4. Conclusions

The spectrum of a C_{60} thin film from 0.6 to 6.5 eV is determined by the combination of PDS with conventional transmission spectroscopy. The weak optical absorption spectra of solid C_{60} are obtained by PDS measurements both for single crystals grown from gas or solution and for polycrystalline thin films. Several features in the weak-absorption region

are strikingly similar to those of amorphous semiconductors. The exponential Urbach tail is attributed to disorder due to unknown impurities or structural defaults. By using a Tauc plot the optical energy gaps are derived as 1.63 eV for a fcc single crystal, 1.65 eV for an orthorhombic single crystal and 1.75 eV for pure thin film. Though both have fcc structure, pure C_{60} single crystal has an optical energy gap that is 0.1 eV smaller than that of pure C_{60} thin film, due to the different degrees of disorder. The optical absorption near the energy gap is extended to the lower-energy side, forming a tail which indicates the existence of some disorder. It is the disorder that causes the difficulty in determination of the energy gap for solid C_{60}. Therefore, it is interesting that the solid C_{60} exhibits a semiconductor-like behaviour in optical absorption properties and yet retains a molecular character.

Acknowledgment

This work was supported by the National Natural Science Foundation of China.

References

[1] Howard J B, McKinnon J T, Makarovsky Y, Lafleur A L and Johnson M E 1991 *Nature* **352** 139
[2] Hare J P, Kroto H W and Taylor R 1991 *Chem. Phys. Lett.* **177** 394
[3] Ajie H, Alvarez M M, Anz S J, Beck R D, Diederich F, Fostiropoulos K, Huffman D R, Krätschmer W, Rubin Y, Schriver K, Sensharma D and Whetten R L 1990 *J. Phys. Chem.* **94** 8630
[4] Krätschmer W, Lamb L D, Fostiropoulos K and Huffman D R 1990 *Nature* **347** 354
[5] Hebard A F, Haddon R C, Fleming R M and Kortan A R 1991 *Appl. Phys. Lett.* **59** 2109
[6] Kelly M K, Etchegoin P, Fuchs D, Krätschmer W and Fostiropoulos K 1992 *Phys. Rev.* B **46** 4963
[7] Skumanich A 1991 *Chem. Phys. Lett.* **182** 486
[8] Wen C, Aida T, Honma I, Komiyama H and Yamada K 1994 *J. Phys.: Condens. Matter* **6** 1603
[9] Matsuura S, Tsuzuki T, Ishiguro T, Endo H, Kikuchi K, Achiba Y and Ikemoto I 1994 *J. Phys. Chem. Solids* **55** 835
[10] Jost M B, Troullier N, Poirier D M, Martins J L, Weaver J H, Chibante L P F and Smalley R E 1991 *Phys. Rev.* B **44** 1966
[11] Mort J, Okumura K and Machonkin M 1991 *Chem. Phys. Lett.* **186** 281
[12] Saito S and Oshiyama A 1991 *Phys. Rev. Lett.* **66** 2637
[13] Yang S H, Pettiette C L, Conceicao J, Cheshnovsky O and Smalley R E 1987 *Chem. Phys. Lett.* **139** 233
[14] Hensen P L, Fallon P J and Krätschmer W 1991 *Chem. Phys. Lett.* **181** 367
[15] Lof R W, van Veenendaal M A, Koopmans B, Jonkman H T and Sawatzky G A 1992 *Phys. Rev. Lett.* **68** 3924
[16] Zhou W Y, Xie S S, Zhang Y L, Wang G, Dong C and Wu F 1995 *Chinese Sci. Bull.* **39** 1665
[17] Kikuchi K, Suzuki S, Saito K, Shiromaru H, Ikemoto I, Achiba Y, Zakhidov A A, Ugawa A, Imaeda K, Inokuchi H and Yakushi K 1991 *Physica* C **185–189** 415
[18] Han D X, Qian S F and Xiao Y 1988 *Wuli* **18** 99 (in Chinese)
[19] Jackson W B, Amer N M, Boccara A C and Fournier D 1981 *Appl. Opt.* **20** 1333
[20] Koruga D, Hameroff S, Withers J, Loutfy R and Sundareshan M 1993 *Fullerene C_{60}* (Amsterdam: Elsevier) p 93
[21] Tauc J 1974 *Amorphous and Liquid Semiconductors* (London: Plenum) pp 159–220